water

MDPI

Article

Application of Hydrological and Hydrogeological Models for Evaluating Groundwater Budget in a Shallow Aquifer in a Semi-Arid Region Under Three Pumping Rate Scenarios (Tavoliere di Puglia, Italy)

Paolo Petio [1], Isabella Serena Liso [1,2,*], Nicola Pastore [3,*], Pietro Pagliarulo [1], Alberto Refice [4], Mario Parise [1,2], Giuseppe Mastronuzzi [1,2], Massimo Angelo Caldara [1] and Domenico Capolongo [1,2]

1 Department of Earth and Environmental Sciences, University Aldo Moro, 70125 Bari, Italy; paolo.petio@uniba.it (P.P.); pietro.pagliarulo@uniba.it (P.P.); mario.parise@uniba.it (M.P.); giuseppe.mastronuzzi@uniba.it (G.M.); massimoangelo.caldara@uniba.it (M.A.C.); domenico.capolongo@uniba.it (D.C.)
2 Interdepartmental Research Center of Coast Dynamic, University Aldo Moro, 70125 Bari, Italy
3 Department of Civil, Environmental and Structural Engineering and Chemistry (DICATECh), Polytechnic of Bari, 70125 Bari, Italy
4 Institute for the Electromagnetic Sensing of the Environment—Italian National Research Council (IREA-CNR), 70125 Bari, Italy; alberto.refice@cnr.it
* Correspondence: isabella.liso@uniba.it (I.S.L.); nicola.pastore@poliba.it (N.P.)

Abstract: We analyze the variation in groundwater budget by modeling an aquifer in a semi-arid region in southern Italy, using different good pumping scenarios. This aquifer is overexploited due to the agricultural vocation of the area. We propose an integrated method to assess the distribution of hydrogeological parameters and the recharge rates. The hydrogeological parametrization is performed through a hydrostratigraphic approach using the geostatistical tool. Recharge rates are computed through a soil water balance application, using different monitoring stations over the area for the whole period of interest. Integrating the results of this analysis with pumping scenarios based on the water irrigation requirement of the main crops in the area, different water budgets are estimated. The results show how different pumping scenarios affect the availability of water resources and thus underline the importance of management. This integrated hydrogeological model can be applied to other areas with similar hydrogeological characteristics, and it can be considered a valuable tool for evaluating sustainable groundwater management strategies, considering land use practices and socio-economic factors.

Keywords: modeling; hydrogeology; soil water balance; groundwater recharge; groundwater exploitation

check for updates

Citation: Petio, P.; Liso, I.S.; Pastore, N.; Pagliarulo, P.; Refice, A.; Parise, M.; Mastronuzzi, G.; Caldara, M.A.; Capolongo, D. Application of Hydrological and Hydrogeological Models for Evaluating Groundwater Budget in a Shallow Aquifer in a Semi-Arid Region Under Three Pumping Rate Scenarios (Tavoliere di Puglia, Italy). *Water* **2024**, *16*, 3253. https://doi.org/10.3390/w16223253

Academic Editors: Juan José Durán and Paula M. Carreira

Received: 14 September 2024
Revised: 6 November 2024
Accepted: 9 November 2024
Published: 12 November 2024

Copyright: © 2024 by the authors. Licensee MDPI, Basel, Switzerland. This article is an open access article distributed under the terms and conditions of the Creative Commons Attribution (CC BY) license (https://creativecommons.org/licenses/by/4.0/).

1. Introduction

In recent years, especially in the Mediterranean area, groundwater over-abstractions have led to significant impacts on both the quantity and quality of underground resources [1,2], driven by increasing freshwater demand for different purposes combined with changes in the precipitation pattern.

Several studies have reported a rise in the frequency and intensity of rainfall events, as well as prolonged droughts, with a noticeable decline in average annual precipitation in the Mediterranean area [3,4]. In this context, coastal aquifers are particularly sensitive to groundwater extraction and shifts in precipitation patterns [5,6].

Groundwater plays a crucial role in the agricultural, industrial, and domestic sectors in both rural and urban areas. Sustainable groundwater management requires a comprehensive understanding of groundwater flow dynamics, including changes in recharge,

discharge, and storage changes [7–9]. It is essential to consider groundwater recharge characteristics, their spatial and temporal variations, and the factors controlling the interaction between surface water and groundwater [10,11].

Integrated hydrogeological models may play an important role in forecasting the effects of human activities, such as groundwater extraction and irrigation, that have the potential to directly impact the hydrogeologic systems [12,13].

One of the key challenges in the hydrogeological model implementation is the definition of a three-dimensional Conceptual Geological Model (CGM) representing the variability of the identified facies. This is necessary to determine the flow units through lateral and vertical integration of the hydraulic properties of the facies. The use of appropriate geostatistical techniques allows the definition of the CGM to respect the available hard and soft data as well as the geological knowledge [14].

At the catchment scale, the assessment of the impact of groundwater pumping scenarios, including numerous discrete groundwater wells and variable pumping rates, poses additional challenges [15]. Land use variability further affects the components of the hydrogeological cycle, influencing components such as irrigation demand, evapotranspiration, and net infiltration due to the change in vegetation [16,17]. A reliable estimation of these components requires the definition of the hydrogeologic balance on a daily scale [18]. Moreover, the hydrogeological model should maintain a low computational cost to allow the implementation of multiple scenarios involving changes deriving from anthropogenic activities and climate [19,20].

In the Mediterranean Basin, the Apulia region in southeastern Italy is highly vulnerable, as it relies almost exclusively on groundwater for all water needs due to the lack of surface waters. A particularly sensitive area is the Cerignola Plain at Tavoliere di Puglia, which is subjected to several natural and anthropogenic stresses, such as sea level rise and consequent shoreline modifications, groundwater pumping from shallow and deep aquifers, and land subsidence [21,22].

In this area, characterized by a semi-arid climate, the shallow aquifer is primarily used for agricultural purposes. Groundwater levels data, collected as part of the Tiziano Project, a monitoring plan for groundwater qualitative and quantitative monitoring funded by the Apulia Region Administration [23], showed a significant decline in the piezometric level of the shallow aquifers between 1950 and 2007, leading to the drying up of many wells. The study area contains a high density of groundwater wells, including both registered (active and abandoned) and non-registered (not authorized) wells.

As regards the groundwater quality, the water chemical composition at Tavoliere di Puglia is highly variable due to the variation in the nature and permeability of the materials composing the aquifer. In particular, the chemical composition of the shallow aquifer is influenced by the interaction processes between the soil matrix, often rich in clay minerals, and the rainwater infiltrating underground; at the coastal zones, the water quality is also affected by seawater intrusion. In general, shallow groundwater has a moderate salinity value of approximately 0.7–0.9 g/L, although in some cases, it can exceed 1 g/L. Only the wells closest to the coastline have higher salinity (about 4 g/L) with sodium-chloride facies determined by marine intrusion [24].

The present study illustrates a physically-based numerical model to assess groundwater dynamics, focusing on precipitation, evapotranspiration, infiltration, and aquifer recharge and discharge in the area. The goal is to understand the aquifer response to increasing pumping rates and to evaluate potential actions for sustainable groundwater management. The methodology employs a hydrologic model (Soil Moisture Balance) paired with a groundwater flow model based on the MODFLOW code.

Following analogous approaches used in similar hydrogeological contexts [25], we apply in this work a methodology based on the discretization of the lithostratigraphy into hydrogeologic units and assess their distribution using a geostatistical method. After defining the hydrogeological parameters and estimating the groundwater recharge, groundwater levels, and total storage were calculated for three different well pumping scenarios.

2. Geological and Hydrogeological Settings

The Cerignola Plain extends for about 1.000 km^2, facing the Adriatic Sea in Apulia (Figure 1). Located in the southern part of the Tavoliere di Puglia plain, it is bounded by the Carapelle torrent to the north, the mountain ridges of the Daunia Apennines to the west, and the Ofanto river to the southeast [26].

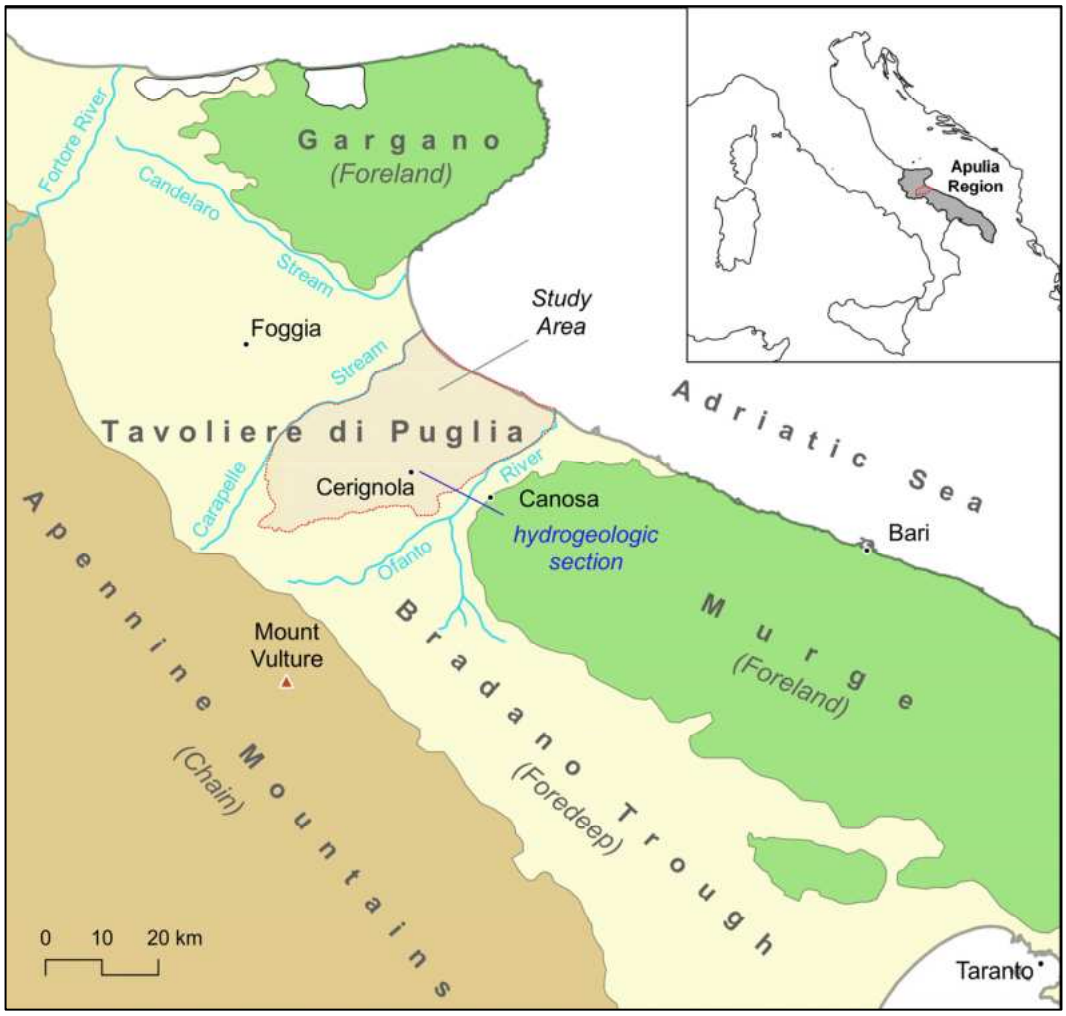


Figure 1. Location of the study area.

The geodynamic evolution of this plain is closely connected to those of the Bradanic trough [27]. Geologically, its formation began during the Lower Pliocene between the southern Apennine chain and the Apulian foreland [28]. The Bradanic trough was affected by two geodynamic phases: the first (Middle Pliocene—Lower Pleistocene) induced intense subsidence over the entire area (estimated at around 2 mm/year), leading to the accumulation of carbonate marine deposits (Calcarenite di Gravina, GRA), followed by silty–clay hemipelagic deposits (Argille subappennine, ASP). The second phase (Middle Pleistocene—present time) is related to a general uplift of the entire Apulian foreland and generated the regressive deposits of the Bradanic trough [29–33].

The study area is characterized by Holocene-Pleistocene deposits belonging to stratigraphic units associated with the second geodynamic phase (Figure 1). The glacio-eustatic sea-level oscillations, occurring simultaneously with regional uplift, added further complexity to the regression mechanism. Consequently, the area is characterized by alternating marine and alluvial terrace deposits. Recently, in the new geological map that covers part of the study area [34], the marine and continental deposits have been included in the domain

of the Bradanic trough, while the alluvial terraces related to the Cervaro and Carapelle streams have been grouped in the Tavoliere di Puglia supersynthem (TP) and the Ofanto river alluvial deposits in the Ofanto river supersynthem (OF), as shown in Figure 2.

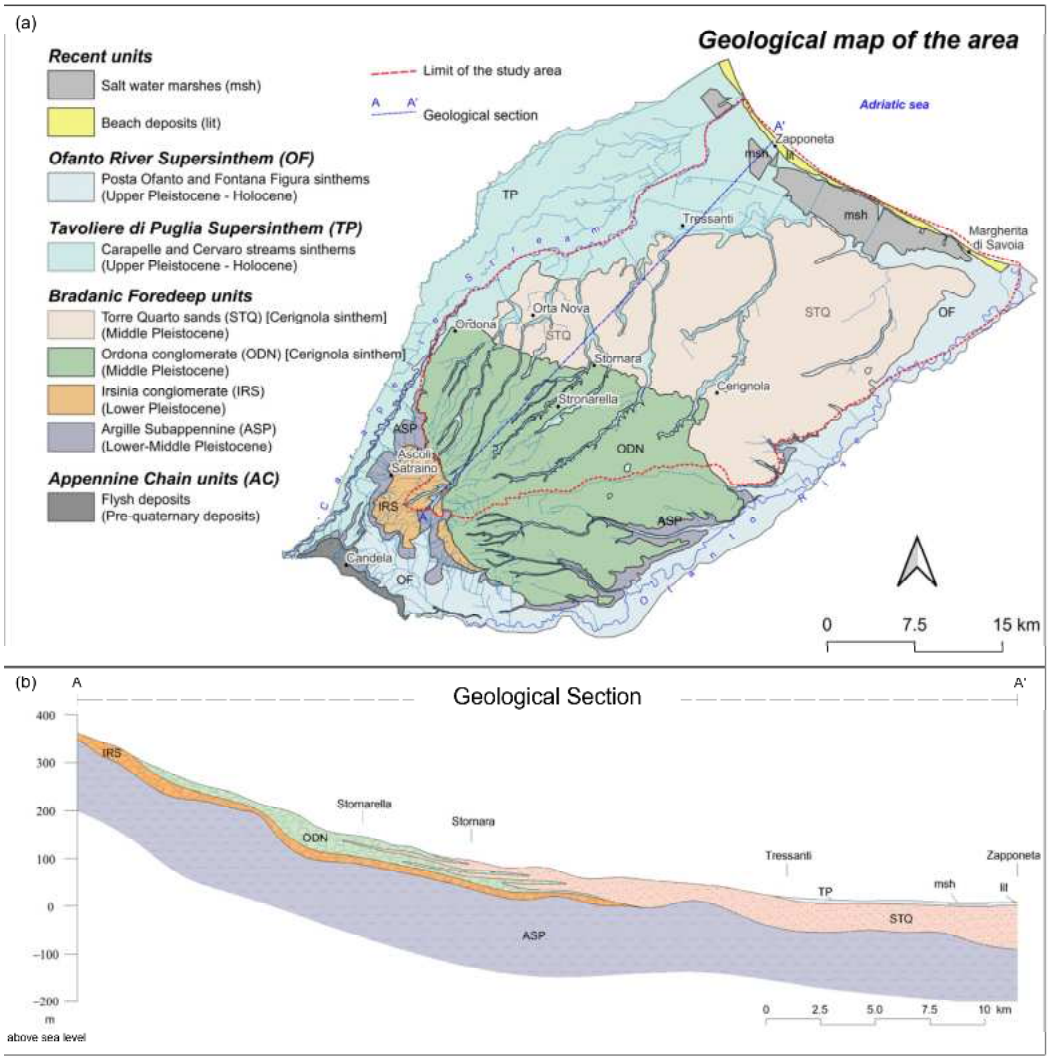


Figure 2. (**a**) Schematic geological map (original surveys by the authors, modified after [34]); (**b**) geological section of the area.

Within the stratigraphy of the Bradanic foredeep, two main discontinuity surfaces have been identified. The first separates the Argille subappennine from the Cerignola synthem, which is attributable to the Middle Pleistocene. This latter represents the most extensively studied deposits in the present research. At the top of the Cerignola synthem, two erosional unconformity boundary surfaces have been identified: the first, partially present in the southeastern sector of the study area, separates the Cerignola synthem deposits from the Ofanto River supersynthems (OF). The second unconformity surface, cropping out at the northwestern sector of the area, constitutes the base of the Tavoliere di Puglia supersynthem (TP) [35,36].

The Cerignola synthem includes two heteropic litho-stratigraphical units: the Ordona conglomerates (ODN), deposited in an alluvial plain, and the Torre Quarto sands (STQ), indicative of various environments, from infralittoral to transitional [35,36].

The geological setting of the study area gives rise to the existence of three different aquifers (Figure 3) hosted within the permeable formations [37,38]. From bottom to top, the sequence is as follows:

- Fractured karst bedrock aquifer;
- Deep porous aquifer;
- Shallow porous aquifer (object of investigation in the present study).

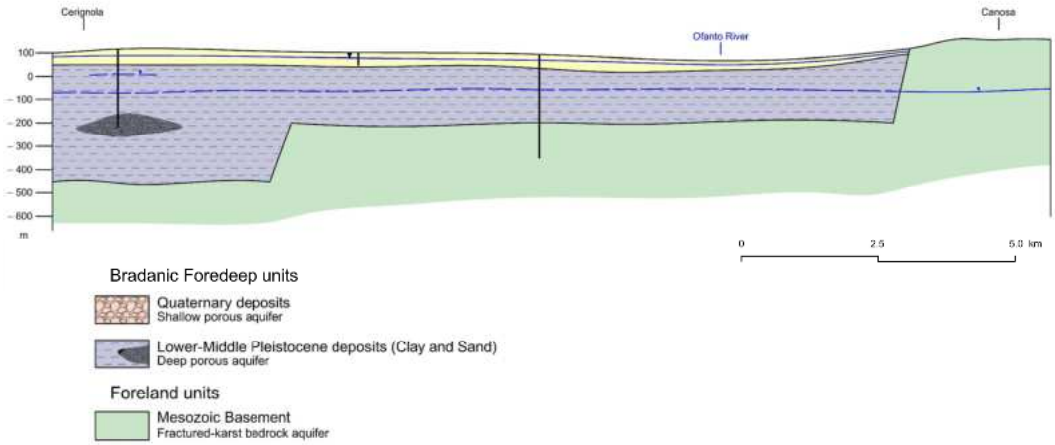


Figure 3. Hydrogeological schematic section of the Tavoliere di Puglia Plain adapted to the Cerignola Sheet of the Geological Map of Italy, scale 1:50,000 (modified after [34]).

2.1. Fractured Aquifer—Karst Bedrock

The groundwater flows within the carbonate rocks of the bedrock and is in continuity with the Murgia karst aquifer. Groundwater circulation is heavily influenced by the fracturing and karstification of the carbonate rock masses [39–41].

2.2. Deep Porous Aquifer

The deep porous aquifer is present in relatively thin silt, sand, and gravel levels interbedded at different depths within the Plio-Pleistocene clay succession. It is a confined aquifer, with piezometric levels rising for hundreds of meters, sometimes above the topographic surface. The spatial distribution, geometry, and hydraulic parameters of these water bodies are still poorly known [42].

2.3. Shallow Porous Aquifer

The shallow porous aquifer occurs in the permeable deposits overlaying the Pleistocene clay formation. Stratigraphic data from the many boreholes drilled in the area show the existence of high permeable sand and gravel levels alternated with silt and clay strata with lower permeability. Groundwater flows in the permeable formations that constitute, in most cases, a unique hydraulically interconnected system. Generally, in the Tavoliere di Puglia innermost areas, more permeable coarse-grained sediments prevail and play a significant role in the aquifer circulation. Toward the coast, less permeable silt and sand intercalations (Late Quaternary) with greater thickness are more frequent, playing the role of aquitards or aquiclude. Inland groundwater presents free flow conditions, whereas it is under pressure towards the coastline, thus inhibiting any interaction with seawater [24,43,44].

The total thickness of the aquifer varies considerably in space, with a general increase from the inner sectors to the coast, where it shows the highest values, about 50 m [45].

Recharge of the aquifer comes from both rain infiltration and the contribution of the Carapelle stream with seasonal variations, while the contribution of the Ofanto River is almost null since it flows in the recessed riverbed, bordered by Argille Subappennine (Plio-Pleistocene). Additional inputs are attributable to irrigation. The outputs, on the other hand, mainly derive from the overexploitation of the groundwater resource by means of pumping wells [24,43].

3. Methods

3.1. Dataset

The stratigraphy of about 300 boreholes for water exploration purposes was collected (Figure 4) to define the geometry and the hydrostratigraphic features of the shallow porous aquifer.

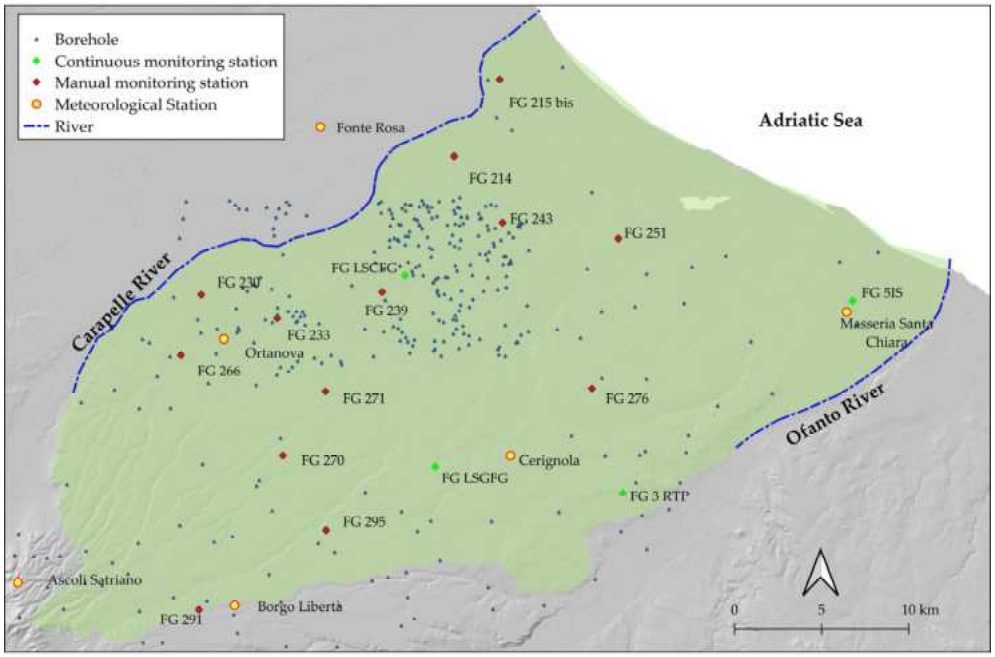


Figure 4. Map showing the ubication of boreholes, meteorological (thermo-pluviometric) gauges, and manual and automatic monitoring stations.

Moreover, daily meteorological data derived from the Regional Service Network of Civil Protection were collected. In detail, six thermo-pluviometric stations were considered in the timespan from February 2011 to June 2021.

To reconstruct the piezometric level and its variation in time, monitoring data retrieved by the Tiziano Project were used. This project, whose purpose was the groundwater qualitative and quantitative assessment, was implemented from the end of 2006 to the first half of 2011, enabling the creation of a widespread monitoring network to improve the region's hydrogeological knowledge [23]. In the study area, 17 stations are present, 13 of them with manual periodic measurements (see Supplementary Materials) and the remaining with continuous monitoring (Figure 5). These data were used for both calibrating the model and validating the results.

3.2. Hydrostratigraphic Analysis

The geological and hydrogeological settings described in previous sections allowed the definition of the shallow porous aquifer conceptual model.

The study area (Figures 1 and 2) is characterized by an extension of about 1000 km^2 and includes almost the entire Cerignola Plain. The southwest edge is characterized by the presence of Argille Subappennine (ASP) at the outcrop, which represents the bottom limit of the model domain [46,47]. The shallow aquifer has been modeled up to this geological layer. Two rivers flow at the borders of the area: the first is the Ofanto River, flowing for about 17 km on the southeastern side; on the northwestern sector, the Carapelle stream borders the area for 38 km. The drainage network shows an intermittent regime, with significant flows for short times after intense and prolonged rainfall.

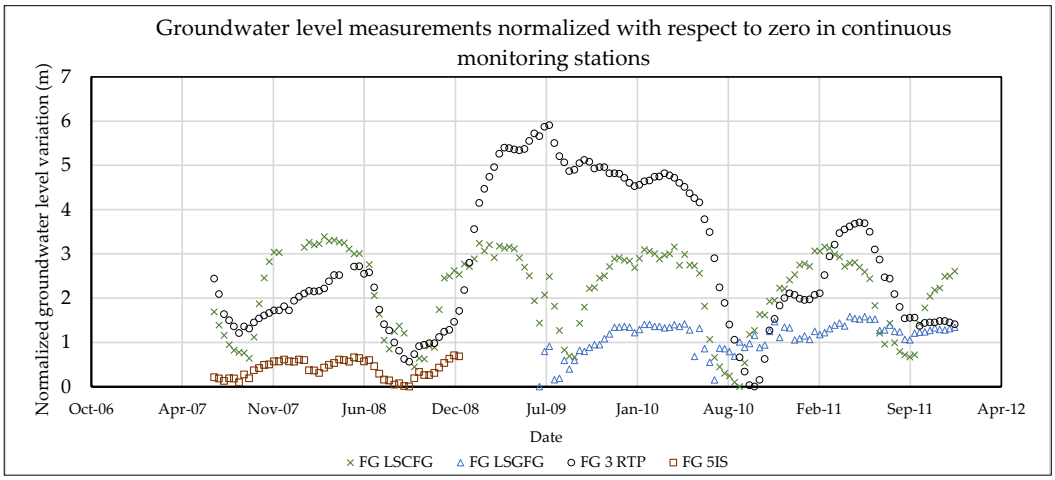


Figure 5. Normalized groundwater level during time in four automatic monitoring stations.

Given the geological complexity and the extent of the study area, it was necessary to adopt a lithology grouping procedure based on the hydrogeological characteristics of the geological formations [48]. Three hydrostratigraphic units with homologous hydrogeological characteristics were defined, grouping silty–sands with sands, silty–clay with clay, and, eventually, conglomerate, thus obtaining the final units: sand, clay, and conglomerate.

A geostatistical approach was adopted to define the spatial variability of the hydrostratigraphic distribution. Specifically, through the Stanford Geostatistical Modeling Software (SGeMS, v2.5b), it was possible to estimate the spatial distribution of the different lithologies, as illustrated in a previous work [25].

Knowing the spatial distribution and the elevation of each borehole, the upper and lower surfaces of the domain were normalized with respect to two horizontal planes. This procedure allowed the indicator kriging to be performed in a three-dimensional grid. Considering the extent of the area and the borehole distribution, the size of each cell was defined as 500 m × 500 m on the horizontal plane and 1.25 m in the vertical direction.

3.3. Hydrologic Balance and Recharge Computation

Groundwater recharge from precipitation was assessed by means of the U.S. Geological Survey Soil–Water Balance (SWB 2.0) code [49]. This tool was developed to estimate net infiltration below the root zone and its variation overtime on a regular grid defined by users. The results can eventually be integrated into MODFLOW. Using readily available data, SWB 2.0 allows us to also calculate other components of the water balance, such as soil moisture, potential and current evapotranspiration, canopy interception, and crop water demand. Based on a modified Thornthwaite–Mather soil–water balance approach [50], the tool computed the net infiltration and the other parameters on a rectangular grid.

In order to perform the computation, SWB 2.0 requires input parameters in grid form, such as hydrologic soil groups, moisture-retaining capacity, available water capacity, flow direction of the drainage network land use, and meteorological data (precipitation and temperature). Furthermore, for each land use class, a crop coefficient has been defined to compute both canopy interception and irrigation values in the period between mid-April and mid-October to evaluate their contribution to the recharge [51].

Hydrologic soil groups, moisture-retaining capacity, available water capacity, and crop coefficient were defined based on the comprehensive analysis of these data for Apulia, as provided in [24].

Land use data for Cerignola Plain were obtained from the CORINE Land Cover database (CLC2018) [52]. A total of 58 Land Cover (LC) classes were identified in the study area, which were reclassified into 12 land use classes for SWB 2.0 input data purposes (Figure 6).

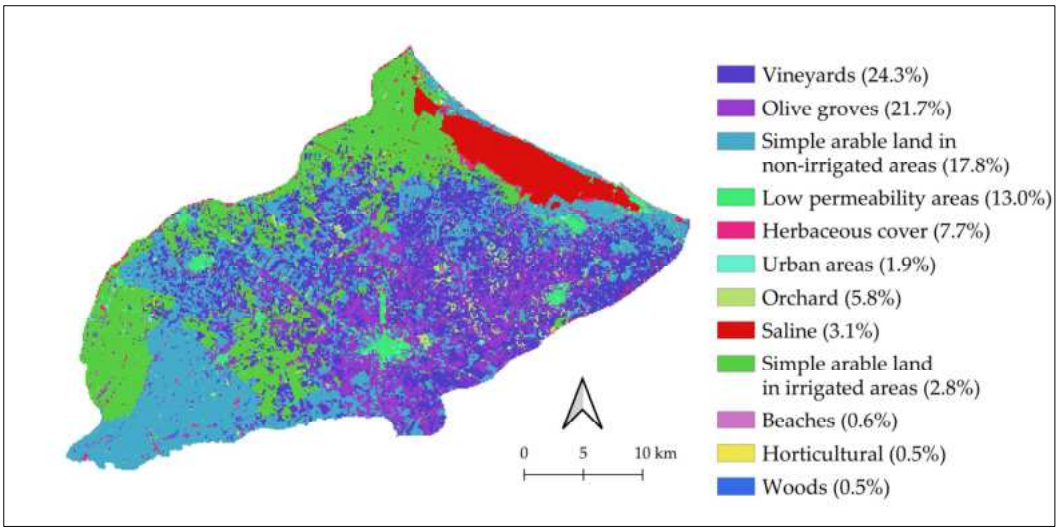


Figure 6. Land use map used for hydrological computation.

Starting from daily records of precipitation (mm) and temperature (°C), an inverse distance weight (IDW) interpolation was performed in MATLAB, obtaining the distribution of the parameters in the whole area using a grid with 74 rows and 108 columns. A raster with 500 m resolution was obtained for each daily time step from 2007 to 2021.

3.4. Hydrogeological Parametrization and Boundary Conditions

To implement the conceptual model and define the initial and boundary conditions, the parameterization of the aquifer was carried out by means of packages integrated into MODFLOW.

A finite difference grid in MODFLOW was used to discretize the study area. The model domain covers an area of 990 km^2 with a regularly spaced grid of 108 columns and 74 rows with a cell size of 500 m $\times$ 500 m.

Vertically, the model consists of a single layer. The layer top elevation was established using a digital terrain model (DTM) from the Apulia Region database [23], while the layer bottom elevation was defined as the top surface of ASP [43].

According to the considerations of the previous sections, along the coastline, no flow condition was imposed because discharge flow towards the sea is limited by the presence of the aquiclude. No flow condition was also imposed inland along the boundary in correspondence with the ASP outcrops and the surficial watershed. The aquifer discharge can occur along the river and the deeper incisions of the hydrographic network. Then, hydraulic head-controlled conditions along the rivers bordering the area were set using the general head package (GHD), and discharge dynamics along the hydrographic network were simulated as drain boundary conditions through the DRN package (Figure 7).

The shallow aquifer is supplied directly by the net infiltration. The results obtained from the SWB 2.0 model were used to define the recharge values by means of the RCH package.

Physical properties required for the model were defined using the layer property flow package (LPF). First, hydraulic conductivity (HC), specific storage (SS), and specific yield (SY) were assigned to each hydrostratigraphic unit, previously defined by geostatistical analysis of the hydrostratigraphic data, based on bibliographic sources (Table 1). Secondly, the physical properties were weighted and averaged along the depth in order to associate a representative value to each cell of the implemented flow model.

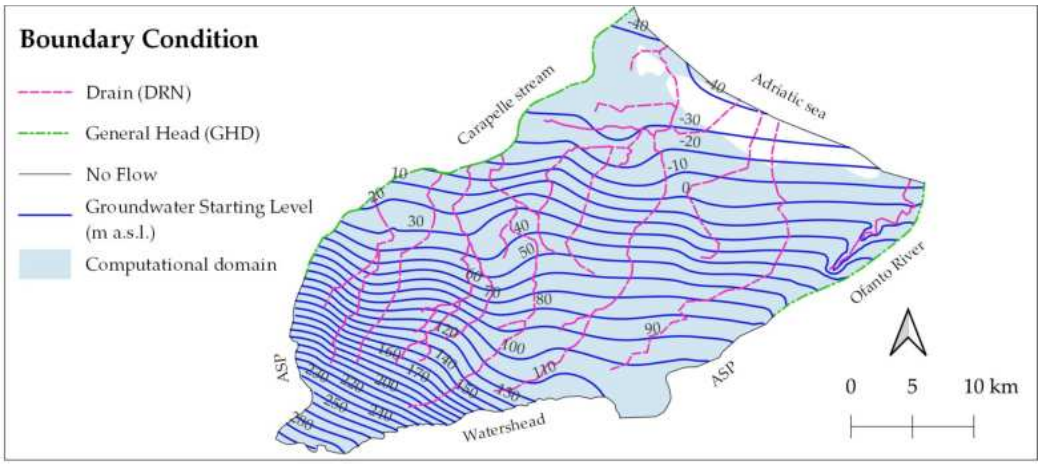


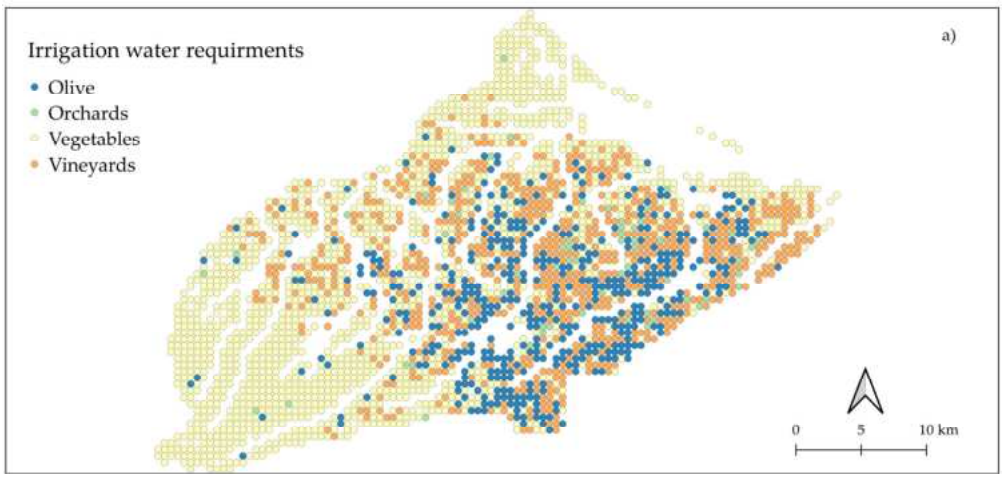
Figure 7. Boundary conditions and starting head.

The starting head was computed through interpolation and comparison of several measurements of piezometric level distributed over the entire area in 2007 with those presented in [24] (Figure 4).

The well density distribution in the Cerignola Plain is very high due to the presence of unauthorized wells. The exact location of the wells and their pumping rate are also difficult to quantify and very uncertain. A spatial well pumping rate was estimated according to the annual irrigation demand for agricultural land use.

Eventually, three scenarios related to the spatial well pumping were defined based on the results obtained by [53], which estimated the irrigation water requirements (IWR) in Apulia for different irrigated crops. Furthermore, in the Foggia province, values related to irrigation water requirement (IWR), irrigation water requirement under controlled deficit irrigation (CDI), and current irrigation water requirement are available.

Then, in each cell of the model, a WELL boundary condition was imposed according to the estimate of the spatial distribution (Figure 8).



b)

Pumping rate ($m^3d^{-1}ha^{-1}$)				
	Olive	**Orchards**	**Vegetables**	**Vineyards**
Full IWR	56.24	109.96	66.77	91.22
IWR CDI	35.02	97.88	60.24	73.21
Act IWR	17.62	94.46	78.45	52.85

Figure 8. (**a**) Crop distribution over MODFLOW grid; (**b**) average values of pumping rate adopted for each crop in the three scenarios: full IWR, requirements under CDI, and actual volumes supplied, all expressed in m^3 per day per ha, in the Foggia province [53].

Moreover, the spatial well pumping rate is not constant during the year, but according to interviews with the locals, the wells are active from mid-April to mid-October, with a peak in July. Then, the temporal variation in the pumping rate during the irrigation season was estimated indirectly by means of the comparison between the observed data and the simulated ones.

Given the huge amount of meteorological data (February 2007–June 2021), to simplify the computation, a time period of 14 years was considered with a time step of 11 days, performing the computation model in a transient regime.

Table 1. Specific storage and specific yield intervals for the main lithologies [54] are used for the implementation of the input data grid throughout the entire domain.

	Specific Storage (1/m)	Specific Yield (%)	Hydraulic Conductivity (m/s)
Gravels	1.5×10^{-5}	25	1.5×10^{-2}
Sands	2.5×10^{-3}	20	7.3×10^{-5}
Clay	2.9×10^{-5}	4	1.7×10^{-9}

4. Results

This chapter summarizes the results obtained from the integrated methodology adopted in this study.

After evaluating the basic statistics for each variable and defining the variogram with the corresponding range and sill (Table 2), three probability distributions were obtained (Figure 9).

The 3D model domain was defined by re-arranging the highest values of probabilities for each of the three variables over the grid and reprojecting it onto the topographic and bottom surfaces (Figure 9d). Comparing this figure with the geological map (Figure 2), a good agreement with the distribution of the lithologies can be appreciated.

Starting from the 3D model obtained combining the probability distribution of the three hydrostratigraphic units, the mean values of hydraulic conductivity, specific storage, and specific yield (Table 1) were assigned to each cell of the domain, and the weighted averages were evaluated along the vertical axis in order to switch from a 3D to a 2D grid.

Figure 10 shows the distribution obtained for the three hydrogeological parameters.

Table 2. Summary of statistics for the three variables and values of sill and range obtained from the horizontal and vertical variograms.

Material	Summary of Statistic			Horizontal Variogram		Vertical Variogram	
	N. of Data	Mean (m)	Variance (m^2)	Sill	Range (m)	Sill	Range (m)
Sand	12,341	0.45	0.25	0.242	1000	0.25	0.55
Clay		0.37	0.23	0.240	1000	0.22	0.23
Congl.		0.19	0.15	0.200	12,000	0.15	0.75

For the GHB package, a specific value for conductance was defined for each arc of the rivers. This boundary condition permits the evaluation of the water exchange between aquifers and rivers.

The results of soil water balance 2.0 are represented in Figure 11. In detail, Figure 11a shows the current evapotranspiration (AET) computed based on the FAO-56 approach [55], assuming that AET and potential evapotranspiration are equal up to some critical soil moisture level. Figure 11b indicates the interception computed by the Bucket method [56], assuming that a constant, user-defined amount of rainfall must occur before any precipitation reaches the soil. Figure 11c, on the other hand, expresses the runoff calculated

by means of the Natural Resources Conservation Service curve number method [57]. Finally, Figure 11d represents the net infiltration based on a modified Thornthwaite–Mather soil–moisture method [50], used as input data in the RCH packages in MODLFOW.

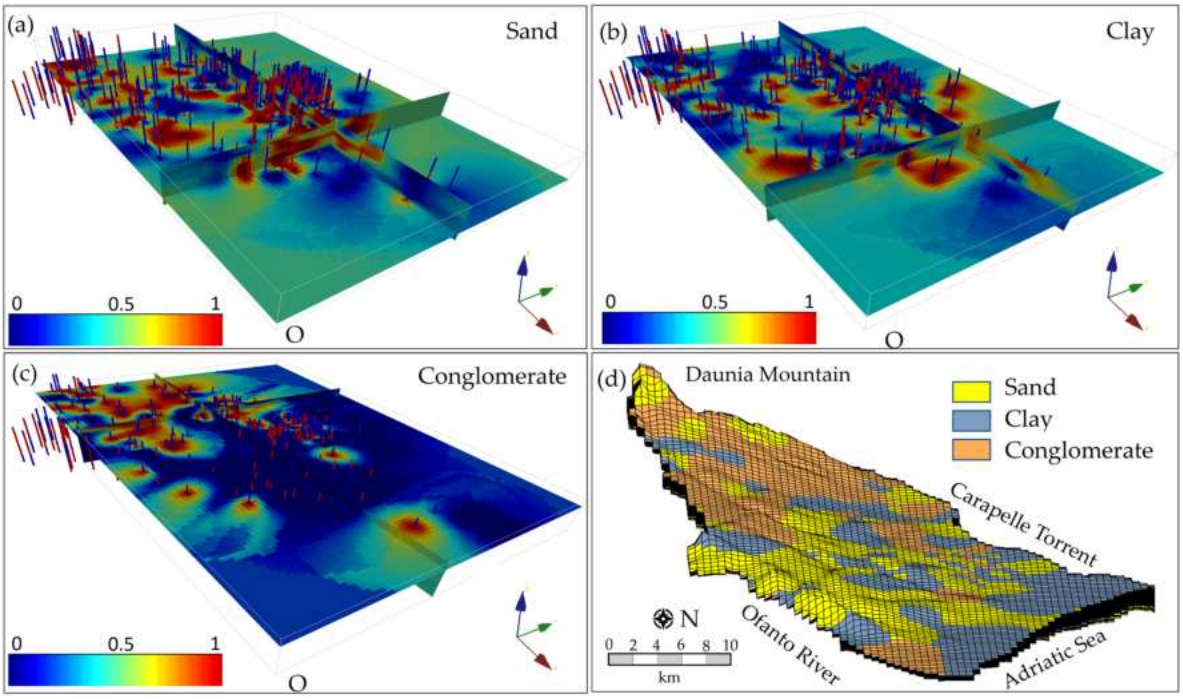


Figure 9. Probabilities distribution for each of the three categorical variables in space, with borehole location: (**a**) sand probabilities distribution; (**b**) clay probabilities distribution; (**c**) conglomerate probabilities distribution; (**d**) 3D model resulting from the combination of the previous probabilities distribution, reprojected onto topographic and bottom surface.

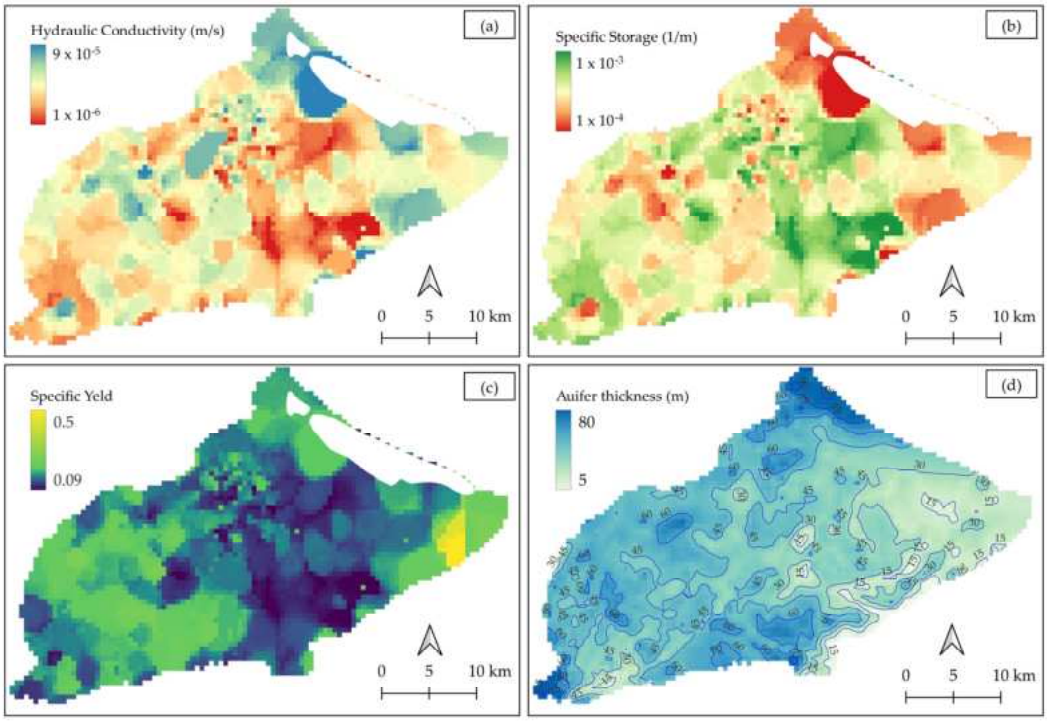


Figure 10. Hydrogeological parameters obtained through geostatistical analysis. (**a**) Hydraulic conductivity (m/s); (**b**) specific storage (m); (**c**) specific yield; (**d**) aquifer thickness (m).

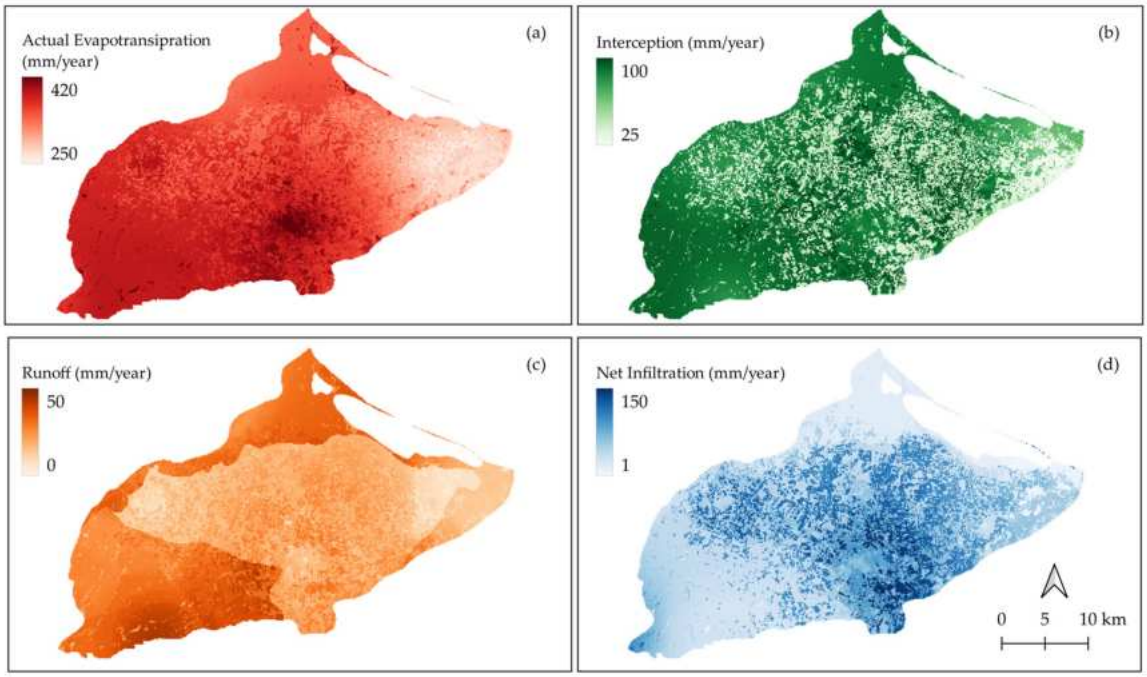


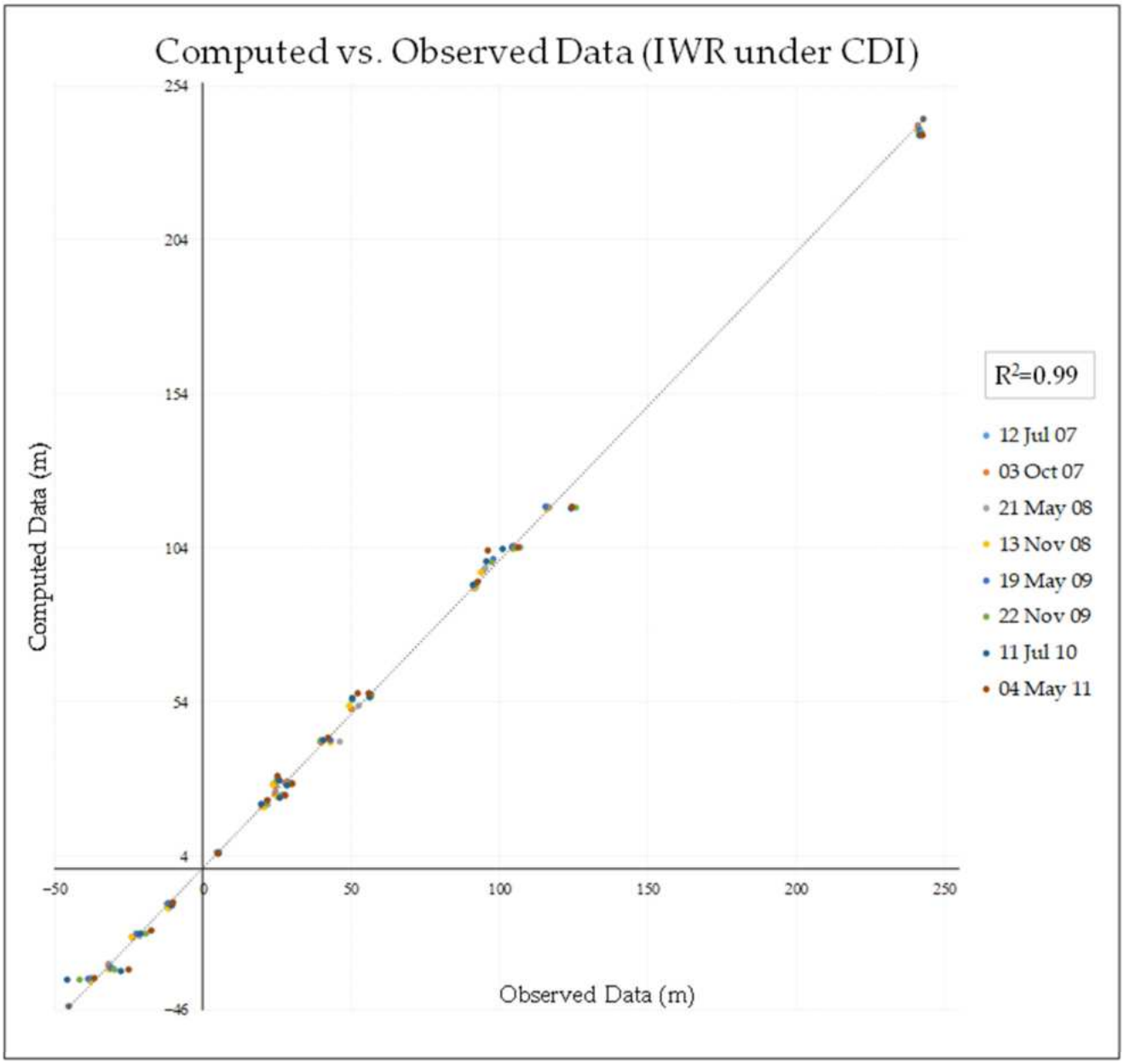
Figure 11. Spatial distribution of average annual soil water balance components: (**a**) Actual evapotranspiration; (**b**) interception; (**c**) surface runoff; (**d**) net infiltration.

These results allow the definition of the hydrogeological model with a transient regime from 2007 to 2021. The groundwater flow and groundwater balance were estimated based on the three scenarios.

In Figure 12, a scatterplot of observed vs. computed values for irrigation water requirement under controlled deficit irrigation is shown, with the statistical summary of residual. This scenario, based on agricultural practices in the area, seems to have a good fit between observed and computed values (mean values of the residuals range from -0.068 m to -1.189 m).

The comparison between observed and computed values of the resulting water flow model for each scenario in continuous monitoring stations is shown in Figure 13. Considering the statistical summary of the residuals (Table 3), the stations showing the best fit are FG 5IS and FG LSCFG, with mean residual values of 0.02 ± 0.33 and 0.06 ± 0.31 for FG 5IS in IWR under ICD and actual IWR scenarios, respectively, and -0.05 ± 0.62 for FG LSCFG in IWR under CDI scenario.

Using the ZONEBUDGET application [58], which calculates the sub-regional water budget on the basis of the results of MODLFOW simulation, computing inflow and outflow for each boundary condition, the hydrogeological balance was estimated for full irrigation water requirement (Full IWR), irrigation water requirement under controlled deficit irrigation (IWR under CDI), and current irrigation water demand (Act IWR). The balance in terms of inflows, outflows, and cumulative storage has been represented in Figure 14.



Statistical Summary of Residual (m)								
Statistics	12 Jul 07	03 Oct 07	21 May 08	13 Nov 08	19 May 09	22 Nov 09	11 Jul 10	04 May 11
	IWR under CDI							
Max	1.877	1.940	3.057	3.212	3.871	5.024	9.165	6.617
Min	-0.712	-1.426	-5.493	-2.574	-4.145	-8.999	-7.783	-8.270
Dev_st	0.843	0.971	2.065	1.873	2.052	3.354	4.062	4.042
Mean	**0.456**	**0.159**	**-1.121**	**-0.445**	**-0.068**	**-0.877**	**-0.182**	**-1.189**

Figure 12. Observed vs. computed data scatterplot for IWR under CDI (agricultural practices) refers to manual station measurements. Summary of statistics referred to residual for IWR under CDI scatterplot.

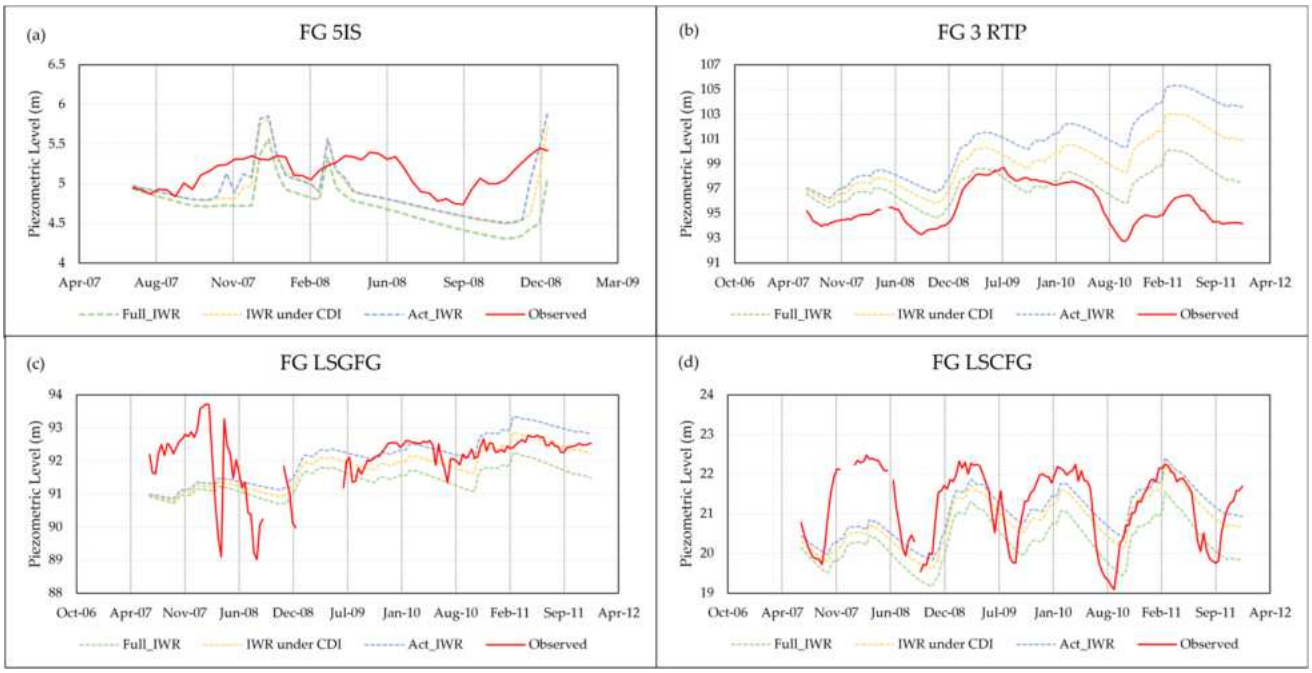


Figure 13. Observed vs. computed graph for each automatic station for each scenario.

Table 3. Summary of statistics of residuals for automatic stations.

Statistical Summary of Residuals (m)												
Statistics	**FG 5IS**			**FG 3RTP**			**FG LSGFG**			**FG LSCFG**		
	Full IWR	IWR Kd	ACT IWR	Full IWR	IWR Kd	ACT IWR	Full IWR	IWR Kd	ACT IWR	Full IWR	IWR Kd	ACT IWR
min	−0.62	−0.86	−0.96	−4.90	−7.84	−10.10	0.96	0.80	0.58	−0.78	−1.43	−1.63
max	0.64	0.46	0.45	0.57	−0.60	−1.06	1.48	1.41	1.34	1.60	1.17	0.94
dev.st	0.27	0.31	0.33	1.31	2.04	2.69	0.15	0.17	0.20	0.56	0.62	0.62
mean	0.23	0.06	0.02	−2.07	−3.99	−5.47	1.21	1.08	0.97	0.48	−0.05	−0.26

The charts are divided in two time steps: the calibrated model from 2006 to 2011 and the forecast model from 2011 to 2021. The first was used to calibrate the hydrogeological parameters and the boundary condition to forecast the water budget under different pumping rate scenarios. The relationship between recharge, discharge, and cumulate storage is evident. Indeed, the discharge rate, influenced by drainage and boundary conditions, increases during the wet season, such as the recharge rate. This latter decreases during the dry season due to aquifer exploitation. This behavior has been observed in every hydrologic year for each scenario.

Finally, Figure 14d summarizes the main differences between each scenario. In the case of Act IWR and IWR under CDI, the cumulate storage does not decrease significantly, whereas, for Full IWR, a high depletion of the aquifer is expected.

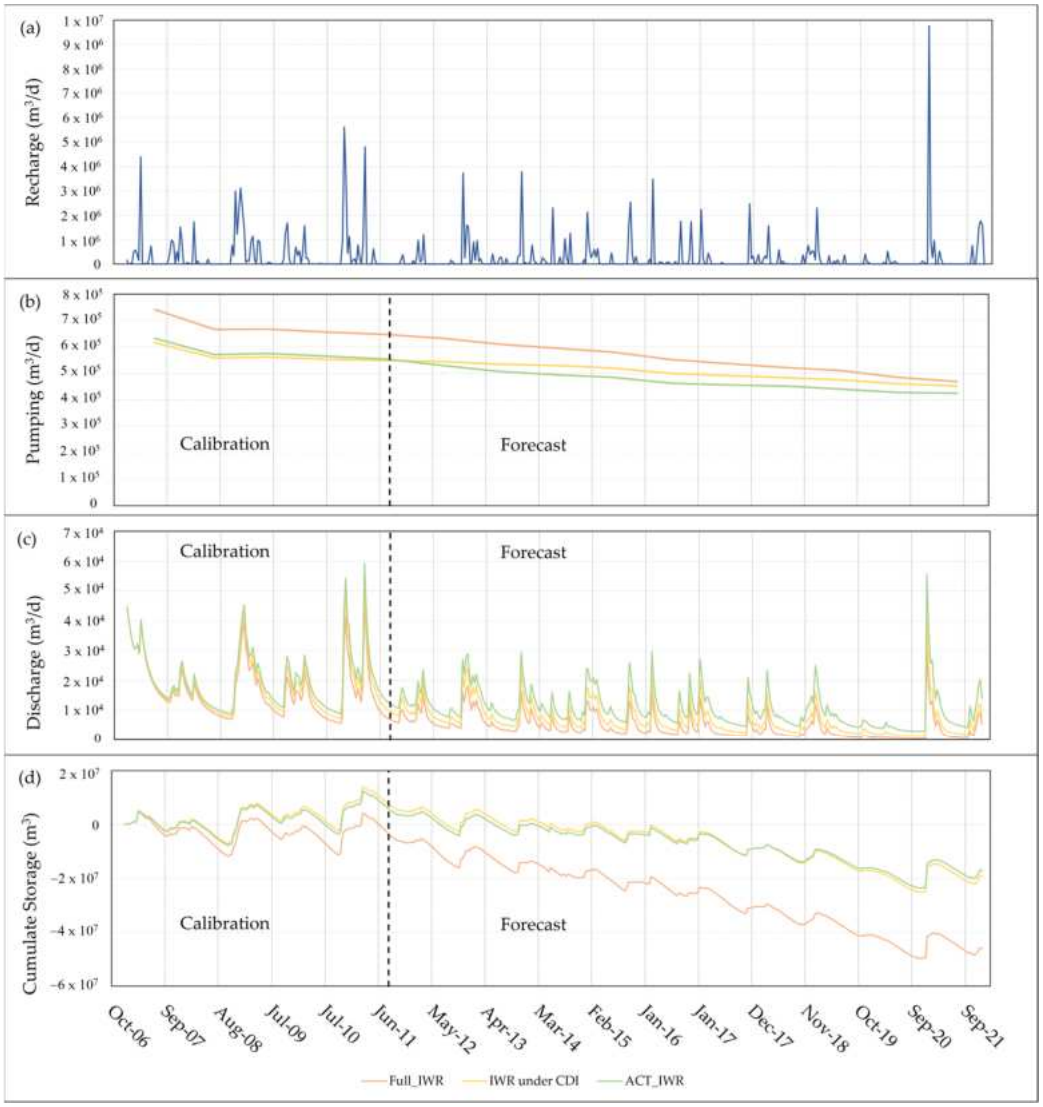


Figure 14. Computed water budget for the three implemented scenarios distinguished between the calibration period and forecast period. (**a**) Recharge of the area in the period considered; (**b**) trend of maximum pumping rate for each scenario; (**c**) discharge for each scenario; (**d**) cumulative storage for each scenario.

5. Discussion

In this study, the impact of pumping scenarios of shallow groundwater resources in the semi-arid region of the Cerignola Plain (Apulia, southern Italy) is investigated. The impact is assessed through the coupling of hydrostratigraphic geostatistical analysis, soil water balance, and groundwater flow models. The modeling framework applied in this study, in comparison with more complex surface–groundwater integrated models, consists of an independent soil water balance model and a groundwater flow model that results more appropriate to achieve the goal of the present study [18,59].

The implementation of the soil water balance separately on a daily scale allowed the analysis of the recharge variation compared to other components such as actual evapotranspiration, surface runoff, and crop interception. For the proposed model, with reliable meteorological data and high-resolution land use information, it was possible to estimate the net infiltration for each land use class based on crop distribution. The results show that main net infiltration occurs over vineyards and orchards in winter, with mean annual values of 100 mm, while in olive groves, simple arable land, and horticultural crops, the contribution is estimated to be in the range of 50–70 mm per year. The comparison between

the net infiltration and the geological map indicates that the main recharge takes place in the central sector of the area, corresponding to the Torre Quarto sands within the Cerignola Synthem, in agreement with what is described by [24]. Furthermore, the hydrologic balance shows that the computed actual evapotranspiration is between 300 and 400 mm for the considered land use classes. Other components that negatively contribute to the recharge include interception and surface runoff. Interception values range from 30 to 170 mm per year, with the highest value corresponding to simple arable land, while runoff shows values between 20 and 50 mm per year, again with maximums recorded in simple arable land. As regards the contribution of irrigation to the aquifer recharge, it has been estimated that the irrigation periods correspond to those with the lowest precipitation (mid-April to mid-October). Therefore, almost all water is absorbed by the crops, with only a minimum amount contributing to the aquifer recharge.

Given the heterogeneity of the sediments in the area due to its geological evolution, a geostatistical approach based on hydrostratigraphic units allowed to obtain a probabilistic distribution of the hydrogeological properties for the entire area, where only limited studies were available [24]. From the results of indicator kriging, the obtained map for hydraulic conductivity, specific yield, and specific storage shows values consistent with those known in the region [24]. Specifically, hydraulic conductivity ranges from 1×10^{-6} to 9×10^{-5} ms^{-1}, specific storage ranges from 0.0001 to 0.001 m^{-1}, while specific yield exhibits low values near 0.09.

The proposed conceptualization of the shallow aquifer in the Cerignola Plain accurately represents the observed groundwater dynamics. The comparison between the observed groundwater level and simulated ones shows a decent fit. The four automatic monitoring stations show different seasonal trends, probably related to the different features of the aquifer and different net infiltration patterns. The model confirms this trend for each station, showing a peak at the end of the winter period and a lowering trend at the end of the summer.

A loss in model reliability is observed along the marginal areas of the model. This is evident in Figure 13, where larger discrepancies occur when there is a lack of data in terms of stratigraphy knowledge or when the groundwater level is more susceptible to river stage. Additionally, in the area with a larger amount of stratigraphic data, the aquifer parameters and the hydrostratigraphic structures are well defined, and as a consequence, the simulation results are more reliable. This study discloses the importance of the definition of the hydrostratigraphic model of the shallow alluvial aquifer to adequately represent the groundwater flow dynamics [60].

The behavior of the aquifer at the boundaries with the Ofanto River and the Carapelle stream shows, in the first case, a trend of the iso-piezometric contours perpendicular to the river, thus underscoring what was stated before about the absence of water exchanges between the aquifer and the river. At the Carapelle stream, the iso-piezometric contours show a parallel trend locally, thus highlighting exchanges between the two systems.

The water budget analysis clearly indicates that drains and rivers play a primary role in the discharge. The hydrographic network of the area is active only during periods of heavy precipitation when the peak corresponds to a high net infiltration event correlated with rainfall. On the other hand, due to the lowering of the water table over time, rivers appear to recharge the aquifer near the coastal plain.

The decision to apply three different pumping scenarios was driven by the need to analyze the roles of well pumping in an area known for its strong agricultural vocation, where aquifer overexploitation is one of the main challenges faced by local farms. Using data related to full irrigation water requirement (full IWR), irrigation water requirement under controlled irrigation demand (IWR under CID), and actual irrigation water requirement (Act IWR), as stated in [53], we defined three scenarios based on crop distribution, assuming no land use change in time.

The results obtained, in terms of cumulative storage, show an initial constant trend related to the observed precipitation patterns during the period 2006–2011, which con-

tributed to a sufficient recharge rate. However, starting in 2011 with the assumption of an equal pumping rate, a depletion of the aquifer is observed in all the scenarios. In the case of IWR under CDI and Act IWR, the decrease in storage is minimal, but the projected model for Full IWR shows a depletion of approximately 5×10^7 m^3. This behavior could be attributed to a decrease in rainfall in recent years, leading to reduced aquifer recharge.

Further, the analyses allowed for a quantitative estimation of the water budget for the investigated area in terms of inflow and outflows under the imposed scenarios until 2021.

6. Conclusions

Managing groundwater resources in a sustainable way is one of the most significant challenges that societies currently face. In this study, for the first time, a methodology aimed at evaluating how variations in well pumping might affect the groundwater resources of the shallow aquifer at the Cerignola Plain was developed and implemented. This was carried out through the application of an integrated method, where each analysis provided useful results for the subsequent evaluations, enabling a reasoned and physically based assessment. Indeed, the evaluation was conducted using numerical models grounded on physical principles, taking into account factors such as soil moisture, the drainage effects of upstream channels, and hydrostratigraphic discretization.

The developed model is a preparatory step for the hydrogeological modeling of the salinization of the aquifers due to the seawater intrusion phenomenon. The study area is affected by saline pollution that can induce progressive deterioration in the quality of the groundwater, likely compromising agricultural activities. Along the coastal area, the direct flow toward the Adriatic Sea is limited. In this zone, the aquifer lies in the sand intercalations at greater depth within the less permeable silts. Therefore, the lateral intrusion phenomenon in the shallow aquifer is limited. In this aquifer, saltwater contamination occurs primarily by means of upconing phenomena as a result of the deepening of wells to exploit the deep carbonate aquifer. The latter, due to its degree of permeability, is affected by lateral seawater intrusion. It is not uncommon to find wells without casing installed in deep aquifers in the study area that could give rise to hydraulic connections between the deep and the shallow aquifers, thus triggering local saline pollution. The accuracy of the groundwater flow model can be further improved by incorporating additional hydrogeological data eventually available and more detailed characters of the shallow aquifer.

The outcomes of this study, notwithstanding the limitations provided by a non-homogenous data coverage, both in spatial terms and in time, represent a useful advancement for the Cerignola Plain in terms of improving the knowledge of the overall situation of the aquifer. For better management of the water resources in the area, several urgent actions should be pursued, as summarized in the following recommendations:

- a wider, more detailed collection and public availability of data about the wells;
- a more efficient control of the territory to prevent the high number of illegal, unauthorized wells in the area, which certainly constitutes a strong drawback when trying to develop any hydrogeological model in such a setting;
- improving the monitoring, with specific reference to deepening the understanding of the relationships between piezometric levels and rainfall events, including the negative effects of climate changes in both the amount and distribution of precipitation;
- dissemination among the local community, and in particular the farmers, about the consequences of groundwater resource overexploitation.

A more realistic appreciation of the whole number of wells at work is also mandatory to possibly provide end users with simple indices to evaluate the negative impacts deriving from excessive pumping from nearby wells, thus stimulating the creation of a network within the local community toward a more sustainable use of the water resources.

In conclusion, efforts should be made to couple the results from scientific approaches and from groundwater monitoring with actions by decision-makers and administrators aimed at raising public awareness about the problem and at looking for more appropriate

solutions on the basis of further implementations of physically based models to assess the quality and quantity of groundwater bodies.

Supplementary Materials: The following supporting information can be downloaded at: https://www.mdpi.com/article/10.3390/w16223253/s1, Table S1: Piezometric level data derived by the Tiziano Project and SIT Puglia website.

Author Contributions: Conceptualization, P.P. (Paolo Petio), I.S.L. and N.P.; methodology, P.P. (Paolo Petio), I.S.L. and N.P.; software, P.P. (Paolo Petio), and N.P.; validation, I.S.L., N.P., M.P., P.P. (Pietro Pagliarulo), and M.A.C.; formal analysis, P.P. (Paolo Petio), I.S.L., N.P. and M.P.; investigation, P.P. (Paolo Petio), and N.P.; resources, P.P. (Paolo Petio), N.P., M.A.C. and M.P.; data curation, P.P. (Paolo Petio); writing—original draft preparation, P.P. (Paolo Petio); writing—review and editing, N.P., I.S.L., P.P. (Pietro Pagliarulo), A.R., M.P., M.A.C. and D.C.; visualization, P.P. (Paolo Petio), N.P. and P.P. (Pietro Pagliarulo); supervision, D.C., M.A.C. and M.P.; project administration, D.C. and M.A.C.; funding acquisition, G.M. All authors have read and agreed to the published version of the manuscript.

Funding: This research received funding from the PRIN 2022 Project GAIA—"Geomorphological and hydrogeological vulnerability of Italian coastal areas in response to sea level rise and marine extreme events" (Project 2022ZSMRXJ P.I.: G. Mastronuzzi), funded by MUR—Ministero dell' Università e Ricerca.

Data Availability Statement: Requests for materials should be addressed to Paolo Petio.

Acknowledgments: This paper collects the results of studies performed in the framework of the PRIN 2022 Project GAIA—"Geomorphological and hydrogeological vulnerability of Italian coastal areas in response to sea level rise and marine extreme events" (Project 2022ZSMRXJ P.I.: G. Mastronuzzi), funded by MUR—Ministero dell' Università e Ricerca. This study was also partly carried out within the RETURN Extended Partnership and received funding from the European Union Next-GenerationEU (National Recovery and Resilience Plan—NRRP, Mission 4, Component 2, Investment 1.3—D.D. 1243 2/8/2022, PE0000005).

Conflicts of Interest: The authors declare no conflicts of interest.

References

1. Tuel, A.; Eltahir, E.A.B. Why is the Mediterranean a climate change hot spot? *J. Clim.* **2020**, *33*, 5829–5843. [CrossRef]
2. Pandey, A.; Padhya, V.; Ganguly, A.; Chakra, S.; Deshpande, R.D. Surface water groundwater interaction in water-stressed semi-arid western India: Insights from environmental isotopes. *J. Arid Environ.* **2023**, *208*, 104879. [CrossRef]
3. Roseto, R.; Dellino, P.; Capolongo, D. Spatial distribution and trend analysis of extreme rainfall time series in Apulia region (Italy). *Phys. Geogr. Quat. Dyn.* **2024**, *46*, 163–177. [CrossRef]
4. Alpert, P.; Ben-Gai, T.; Baharad, A.; Benjamini, Y.; Yekutieli, D.; Colacino, M.; Diodato, L.; Ramis, C.; Homar, V.; Romero, R.; et al. The paradoxical increase of Mediterranean extreme daily rainfall in spite of decrease in total values. *Geophys. Res. Lett.* **2002**, *29*, 1536. [CrossRef]
5. Davamani, V.; John, J.E.; Poornachandhra, C.; Gopalakrishnan, B.; Arulmani, S.; Parameswari, E.; Santhosh, A.; Srinivasulu, A.; Lal, A.; Naidu, R. A Critical Review of Climate Change Impacts on Groundwater Resources: A Focus on the Current Status, Future Possibilities, and Role of Simulation Models. *Atmosphere* **2024**, *15*, 122. [CrossRef]
6. Crosbie, R.S.; Scanlon, B.R.; Mpelasoka, F.S.; Reedy, R.C.; Gates, J.B.; Zhang, L. Potential climate change effects on groundwater recharge in the High Plains Aquifer, USA. *Water Resour. Res.* **2013**, *49*, 3936–3951. [CrossRef]
7. Raheem, A.; Ahmad, I.; Arshad, A.; Liu, J.; Rehman, Z.U.; Shafeeque, M.; Rahman, M.M.; Saifullah, M.; Iqbal, U. Numerical Modeling of Groundwater Dynamics and Management Strategies for the Sustainable Groundwater Development in Water-Scarce Agricultural Region of Punjab, Pakistan. *Water* **2024**, *16*, 34. [CrossRef]
8. Griffiths, J.; Yang, J.; Woods, R.; Zammit, C.; Porhemmat, R.; Shankar, U.; Rajanayaka, C.; Ren, J.; Howden, N. Parameterization of a National Groundwater Model for New Zealand. *Sustainability* **2023**, *15*, 13280. [CrossRef]
9. Petersen-Perlman, J.D.; Aguilar-Barajas, I.; Megdal, S.B. Drought and groundwater management: Interconnections, challenges, and policy responses. *Curr. Opin. Environ. Sci. Health* **2022**, *28*, 100364. [CrossRef]
10. Bear, J. *Dynamics of Fluids in Porous Media*, 1st ed.; Dover Publications, Inc.: New York, NY, USA, 1972; p. 764.
11. Gumuła-Kawecka, A.; Jaworska-Szulc, B.; Szymkiewicz, A.; Gorczewska-Langner, W.; Pruszkowska-Caceres, M.; Angulo-Jaramillo, R.; Šimunek, J. Estimation of groundwater recharge in a shallow sandy aquifer using unsaturated zone modeling and water table fluctuation method. *J. Hydrol.* **2022**, *605*, 127283. [CrossRef]
12. Barthel, R.; Banzhaf, S. Groundwater and surface water interaction at the regional-scale—A review with focus on regional integrated models. *Water Resour. Manag.* **2016**, *30*, 1–32. [CrossRef]

13. Ponprasit, C.; Zhang, Y.; Gu, X.; Goodliffe, A.M.; Sun, H. Assessing Vulnerability of Regional-Scale Aquifer-Aquitard Systems in East Gulf Coastal Plain of Alabama by Developing Groundwater Flow and Transport Models. *Water* **2023**, *15*, 1937. [CrossRef]
14. Cavero, J.; Orellana, N.H.; Yemez, I.; Singh, V.; Izaguirre, E. Importance of conceptual geological models in 3D reservoir modelling. *First Break* **2016**, *37*, 39–49. [CrossRef]
15. Brookfield, A.E.; Zipper, S.; Kendall, A.D.; Ajami, H.; Deines, J.M. Estimating groundwater pumping for irrigation: A method comparison. *Groundwater* **2023**, *62*, 15–33. [CrossRef]
16. Neukum, C.; Morales Santos, A.G.; Ronelngar, M.; Vassolo, S. Modelling groundwater recharge, actual evaporation and transpiration in semi-arid sites of the Lake Chad Basin: The role of soil and vegetation on groundwater recharge. *Hydrol. Earth Syst. Sci. Discuss.* **2021**, 1–27. [CrossRef]
17. Diouf, O.C.; Weihermüller, L.; Diedhiou, M.; Vereecken, H.; Faye, S.C.; Faye, S.; Sylla, S.N. Modelling groundwater evapotranspiration in a shallow aquifer in a semi-arid environment. *J. Hydrol.* **2020**, *587*, 124967. [CrossRef]
18. Pastore, N.; Cherubini, C.; Giasi, C.I. Integrated Hydrogeological Modelling for Sustainable Management of the Brindisi Plain Aquifer (Southern Italy). *Water* **2023**, *15*, 2943. [CrossRef]
19. Pastore, N.; Cherubini, C.; Doglioni, A.; Giasi, C.I.; Simeone, V. Modelling of the Complex Groundwater Level Dynamics during Episodic Rainfall Events of a Surficial Aquifer in Southern Italy. *Water* **2020**, *12*, 2916. [CrossRef]
20. Rushton, K.R.; Eilers, V.H.M.; Carter, R.C. Improved soil moisture balance methodology for recharge estimation. *J. Hydrol.* **2006**, *318*, 379–399. [CrossRef]
21. Triggiani, M.; Refice, A.; Capolongo, D.; Bovenga, F.; Caldara, M. *Investigation of Subsidence in the Manfredonia Gulf (Southern Italy) Through Multitemporal DInSAR Techniques*; EGU General Assembly: Wien, Austria, 2009.
22. Scardino, G.; Anzidei, M.; Petio, P.; Serpelloni, E.; De Santis, V.; Rizzo, A.; Liso, S.I.; Zingaro, M.; Capolongo, D.; Vecchio, A.; et al. The Impact of Future Sea-Level Rise on Low-Lying Subsiding Coasts: A Case Study of Tavoliere Delle Puglie (Southern Italy). *Remote Sens.* **2022**, *14*, 4936. [CrossRef]
23. SIT Puglia. Available online: http://www.sit.puglia.it (accessed on 10 October 2024).
24. Cotecchia, V. Le acque sotterranee e l'intrusione marina in Puglia: Dalla ricerca all'emergenza nella salvaguardia della risorsa. *Mem. Descr. Carta Geol. D'Ital.* **2014**, *92*, 1228.
25. Cherubini, C.; Giasi, C.; Fausta, M.; Pastore, N. Modeling of the Natural Attenuation through multivariate geostatistical techniques. *Rend. Online Soc. Geol. Ital.* **2009**, *6*, 157–158.
26. Boenzi, F.; Caldara, M.; Capolongo, D.; Dellino, P.; Piccarreta, M.; Simone, O. Late Pleistocene—Holocene landscape evolution in fossa Bradanica, Basilicata (southern Italy). *Geomorphology* **2008**, *102*, 297–306. [CrossRef]
27. Tropeano, M.; Caldara, M.A.; De Santis, V.; Festa, V.; Parise, M.; Sabato, L.; Spalluto, L.; Francescangeli, R.; Iurilli, V.; Mastronuzzi, G.A.; et al. Geological uniqueness and potential geotouristic Appeal of Murge and Premurge, the first territory in Puglia (Southern Italy) aspiring to become a UNESCO Global Geopark. *Geosciences* **2023**, *13*, 131–148. [CrossRef]
28. Ricchetti, G.; Ciaranfi, N.; Luperto Sinni, E.; Mongelli, F.; Pieri, P. Geodinamica ed evoluzione sedimentaria e tettonica dell'avampaese apulo. *Mem. Soc. Geol. Ital.* **1992**, *41*, 57–82.
29. Caldara, M.; Pennetta, L.; Simone, O. Holocene Evolution of the Salpi Lagoon (Puglia, Italy). *J. Coast. Res.* **2002**, *36*, 124–133. [CrossRef]
30. De Santis, V.; Caldara, M.; Torres, T.; Ortiz, J.E. Two Middle Pleistocene Warm Stages in the Terrace Deposits of the Apulia Region (Southern Italy). *Quat. Int.* **2014**, *332*, 2–18. [CrossRef]
31. Patacca, E.; Scandone, P. Post-Tortonian mountain building in the Apennines. The role of the passive sinking of a relic lithospheric slab. In *The Lithosphere in Italy: Advances in Earth Science Research*; Boriani, A., Bonafede, M., Vai, G.B., Eds.; Accademia nazionale dei Lincei: Roma, Italy, 1989; Volume 80, pp. 157–176.
32. Doglioni, C.; Mongelli, F.; Pieri, P. The Puglia uplift (SE Italy): An anomaly in the foreland of the Apenninic subduction due to buckling of a thick continental lithosphere. *Tectonics* **1994**, *13*, 1309–1321. [CrossRef]
33. Doglioni, C.; Tropeano, M.; Mongelli, F.; Pieri, P. Middle–late Pleistocene uplift of Puglia: An anomaly in the Apenninic foreland. *Mem. Soc. Geol. Ital.* **1996**, *51*, 101–117.
34. Caldara, M.; Capolongo, D.; Del Gaudio, V.; De Santis, V.; Pennetta, L.; Maiorano, P.; Simone, O.; Vitale, G. *Note illustrative della Carta Geologica d'Italia Alla Scala 1:50.000 Foglio, 422 "Cerignola"*; Servizio Geologico d'Italia: Ispra, Italy, 2011.
35. De Santis, V.; Caldara, M.; Pennetta, L.; Torres, T.; Ortiz, J.E. Unconformity-Bounded Stratigraphic Units (UBSUs) in an Italian Alluvial-Plain Area: Recognizing and Dating. *J. Sediment. Res.* **2013**, *83*, 96–114. [CrossRef]
36. De Santis, V.; Caldara, M.; de Torres, T.; Ortiz, J.E. Stratigraphic Units of the Apulian Tavoliere Plain (Southern Italy): Chronology, Correlation with Marine Isotope Stages and Implications Regarding Vertical Movements. *Sediment. Geol.* **2010**, *228*, 255–270. [CrossRef]
37. Maggiore, M.; Nuovo, G.; Pagliarulo, P. Caratteristiche idrogeologiche e principali differenze idrochimiche delle falde sotterranee del Tavoliere di Puglia. *Mem. Soc. Geol. Ital.* **1996**, *51*, 669–684.
38. Maggiore, M.; Masciale, R.; Massari, R.; Pappagallo, G.; Passarella, G.; Vurro, M. Caratteri idrostrutturali del Tavoliere di Puglia ed elaborazione di una carta geolitologica a finalità idrogeologiche. *Geol. E Territ.* **2004**, *2*, 6–16.
39. Liso, I.S.; Parise, M. Apulian karst springs: A review. *J. Environ. Sci. Eng. Technol.* **2020**, *8*, 63–83. [CrossRef]
40. Parise, M. Elementi di geomorfologia carsica della Puglia. In *Atti del 45° Corso CNSS-SSI di III Livello di Geomorfologia Carsica*; Parise, M., Inguscio, S., Marangella, A., Eds.; ISPRA: Ispra, Italy, 2008; pp. 93–118.

41. Parise, M. Surface and subsurface karst geomorphology in the Murge (Apulia, southern Italy). *Acta Carsologica* **2011**, *40*, 79–93. [CrossRef]
42. Cotecchia, V.; Ferrari, G.; Fidelibus, M.D.; Polemio, M.; Tadolini, T.; Tulipano, L. Considerazioni sull'origine e rinnovabilità delle acquee presenti in livelli sabbiosi profondi del Tavoliere di Puglia. *Suppl. Quad. Geol. Appl.* **1995**, *1*, 1163–1173.
43. Cotecchia, V. Gli aspetti idrogeologici del Tavoliere delle Puglie. *L'Acqua* **1956**, *11–12*, 168–180.
44. Passarella, G.; Barca, E.; Sollitto, D.; Masciale, R.; Bruno, D.E. Cross-Calibration of Two Independent Groundwater Balance Models and Evaluation of Unknown Terms: The Case of the Shallow Aquifer of "Tavoliere di Puglia" (South Italy). *Water Resour. Manag.* **2017**, *31*, 327–340. [CrossRef]
45. Colacicco, G. La carta delle acque sotterranee del Tavoliere- osservazioni e perforazioni eseguite nel biennio 1951–1952, Consorzio per la Bonifica della Capitanata, Foggia, 1953, 128p.
46. Caldara, M.; Pennetta, L. Nuovi dati per la conoscenza geologica e morfologica del Tavoliere di Puglia. *Bonifica* **1993**, *8*, 25–42.
47. Caldara, M.; Pennetta, L. Pleistocenic buried abrasion platforms in southeastern "Tavoliere" (Apulia, South Italy). Giornate di studio sul tema "Terrazzi marini e linee di costa pleistoceniche". *Il Quat.* **1991**, *4*, 303–309.
48. Goldscheider, N.; Drew, D. Methods in Karst Hydrogeology. In *IAH: International Contributions to Hydrogeology*, 1st ed.; CRC Press: Boca Raton, FL, USA, 2007; Volume 26. [CrossRef]
49. Westenbroek, S.M.; Engott, J.A.; Kelson, V.A.; Hunt, R.J. *SWB Version 2.0—A Soil-Water-Balance Code for Estimating Net Infiltration and Other Water-Budget Components*; U.S. Geological Survey Techniques and Methods: Reston, VA, USA, 2018; Book 6, Chapter A59; p. 118. [CrossRef]
50. Thornthwaite, C.W.; Mather, J.R. The water balance. *Climatology* **1955**, *8*, 185–311.
51. Lamaddalena, N.; Caliandro, A. Riorientamenti produttivi del territorio agricolo pugliese per uno sviluppo rurale sostenibile. In *Promozione di Servizi Orientati Allo Sviluppo Agricolo—Azione 3. Ideaprint*; Almastart: Bari, Italy, 2008; Volume 93.
52. Copernicus Land Monitoring Services. Available online: https://land.copernicus.eu/en/products/corine-land-cover/clc2018 (accessed on 5 September 2024).
53. Matarrese, A.M.S. Evaluation of crop irrigation water requirements in the Apulia region. Master's Thesis, Facoltà di Agraria, University of Bari Aldo Moro, Bari, Italy, 2008.
54. Kuang, X.; Jiao, J.J.; Zheng, C.; Cherry, J.A.; Li, H. A review of specific storage in aquifers. *J. Hydrol.* **2020**, *581*, 124383. [CrossRef]
55. Allen, R.G.; Pereira, L.S.; Raes, D.; Smith, M. Crop evapotranspiration—Guidelines for computing crop water requirements. *FAO Irrig. Drain. Pap.* **1998**, *56*, 174.
56. Lundberg, A.; Eriksson, M.; Halldin, S.; Kellner, E.; Seibert, J. New approach to the measurement of interception evaporation. *Am. Meteorol. Soc.* **1997**, *14*, 1023–1035. [CrossRef]
57. Garen, D.C.; Moore, D.S. Curve Number Hydrology in Water Quality Modeling: Uses, Abuses, and Future Directions. *J. Am. Water Resour. Assoc.* **2005**, *41*, 377–388. [CrossRef]
58. Harbaugh, A.W. *A Computer Program for Calculating Subregional Water Budgets Using Results from the U.S. Geological Survey Modular Three-Dimensional Ground-Water Flow Model 1996*; U.S. Geological Survey: Reston, VA, USA, 1996.
59. Larva, O.; Brki'c, Ž.; Briški, M.; Seidenfaden, I.K.; Koch, J.; Stisen, S.; Refsgaard, J.C. An ensemble approach for predicting future groundwater levels in the Zagreb aquifer impacted by both local recharge and upstream river flow. *J. Hydrol.* **2022**, *613*, 128433. [CrossRef]
60. Cianflone, G.; Vespasiano, G.; De Rosa, R.; Dominici, R.; Apollaro, C.; Vaselli, O.; Pizzino, L.; Tolomei, C.; Capecchiacci, F.; Polemio, M. Hydrostratigraphic Framework and Physicochemical Status of Groundwater in the Gioia Tauro Coastal Plain (Calabria—Southern Italy). *Water* **2021**, *13*, 3279. [CrossRef]

Disclaimer/Publisher's Note: The statements, opinions and data contained in all publications are solely those of the individual author(s) and contributor(s) and not of MDPI and/or the editor(s). MDPI and/or the editor(s) disclaim responsibility for any injury to people or property resulting from any ideas, methods, instructions or products referred to in the content.